Available online at www.sciencedirect.com
ScienceDirect
Physica B 387 (2007) 167–171
PHYSICA B
www.elsevier.com/locate/physb

Electrically controlled dispersion in a nematic cell

Carlos I. Mendoza[a,*], J.A. Olivares[b], J.A. Reyes[c]

[a]Instituto de Investigaciones en Materiales, Universidad Nacional Autónoma de México, Apdo. Postal 70-360, 04510 México, D.F., Mexico
[b]Centro de Investigación en Polímeros, COMEX, Blvd. M. Avila Camacho 138, PH1 y 2, Lomas de Chapultepec 11560, México, D.F., Mexico
[c]Instituto de Física, Universidad Nacional Autónoma de México, Apdo. Postal 20-364, 01000 México, D.F., Mexico

Received 2 February 2006; received in revised form 31 March 2006; accepted 31 March 2006

Abstract

In this work, we show theoretically how the trajectories of a propagating optical beam traveling in a planar-homeotropic hybrid nematic crystal cell depend on the wavelength of the optical beam. We apply a uniform electric field perpendicular to the cell to modify these trajectories. The influence of both, the electric field intensity and the refraction index dependence on the wavelength, give rise to an electrically tuned dispersion that may be useful for practical applications.

PACS: 42.70.Df; 61.30.Gd; 42.15.−i; 78.20.ci

Keywords: Geometrical optics; Liquid crystals; Hybrid cells; Electric fields; Total internal reflection

1. Introduction

Conventional instruments designed to separate light into their chromatic components are based on the dispersion phenomena that can be produced either, by a set of prisms or by a periodical media such as diffraction gratings that amplify the difference between the optical paths of the chromatic components coming from a polychromatic beam. For the first case, the wavelength selection depends on the geometry of the arrangement given by a combination of prisms and apertures that have to be rotated to select the desired wavelength. Similar procedures have to be used for the diffraction grating where the spatial resolution of the device depends on the shape and periodicity of the diffraction grating and also on the materials used to fabricate them [1].

In recent years, liquid-crystal technology has been applied to fabricate diffraction gratings that can modulate the diffraction efficiency through the use of electric fields [2] which distort the orientational configuration of the liquid crystal by producing a modulation of the refractive index. However, this technology has the disadvantage of giving a different direction for each outgoing chromatic component. This fact compels the user to rotate the system for having a normally incident beam on a CCD detector for maximizing the signal.

Liquid crystals are anisotropic materials that can be used to produce a continuous gradient of refractive index by a proper treatment of their confining surfaces. These surface-induced gradients can be controlled by the application of electric or magnetic fields. It has been shown [3] that for a monochromatic beam impinging obliquely onto a nematic hybrid cell, the optical range can reach lengths several times larger than the cell's thickness. Hence, it is possible to use it as a dispersive media similar to the glass prism. In contrast to the devices discussed above, this nematic slab has the advantage that all the outgoing beams corresponding to different wavelengths will emerge parallel to each other. Furthermore, since the orientation can be controlled by electric fields, it is possible to electrically manipulate the thickness of a polychromatic beam to tune the resolution of the device.

In this work, we calculate the optical path for a polychromatic beam and show how the dispersion phenomenon occurring inside the nematic cell could be used to

*Corresponding author. Tel.: +52 55 56224644; fax: +52 55 56161201.
E-mail address: cmendoza@iim.unam.mx (C.I. Mendoza).

0921-4526/$ - see front matter © 2006 Elsevier B.V. All rights reserved.
doi:10.1016/j.physb.2006.03.100

develop a practical scheme to split light into their chromatic components based on the electrically controlled dispersion we present here.

2. Calculation

The system under study consists of a pure thermotropic nematic confined between two parallel substrates with refraction indices N_t and N_b, respectively, as shown in Fig. 1. The cell thickness, l, measured along the z-axis, is small compared to the dimension, L, of the cell plates. The director's initial configuration is spatially homogeneous along the plane x–y and varies with z as given by

$$\hat{\mathbf{n}} = [\sin\theta(z), 0, \cos\theta(z)], \tag{1}$$

which satisfies the hybrid boundary conditions

$$\theta(z=0) = 0,$$

$$\theta(z=l) = \frac{\pi}{2}, \tag{2}$$

where $\theta(z)$ is the orientational angle defined with respect to the z-axis.

A low-frequency uniform electric field E_0, parallel to the z-axis is applied. Then, the equilibrium orientational configurations of the director's field are specified by minimizing the total Helmholtz free energy functional as shown in Ref. [4]. We consider a uniaxial medium for which the dielectric tensor ε_{ij} has the general form

$$\varepsilon_{ij} = \varepsilon_\perp \delta_{ij} + \varepsilon_a n_i[\theta(z)] n_j[\theta(z)], \tag{3}$$

where $\varepsilon_\perp$ and $\varepsilon_\parallel$ are the dielectric constants perpendicular and parallel to the director and $\varepsilon_a \equiv \varepsilon_\parallel - \varepsilon_\perp$ is the dielectric anisotropy. Also, we shall assume the equal elastic constants approximation in which the elastic constants associated with the splay, twist, and bend deformations are described by a single constant K. Then, the free energy functional turns out to be [4]

$$F = \int_V \mathrm{d}V \left[\frac{1}{2} K \left(\frac{\mathrm{d}\theta}{\mathrm{d}z} \right)^2 - \frac{E_0^2}{8\pi} (\varepsilon_\perp + \varepsilon_a \cos^2\theta(z)) \right]. \tag{4}$$

The first and second terms of this equation represent the elastic and electromagnetic contribution of the free energy densities, respectively. The stationary configuration is then obtained from the corresponding Euler–Lagrange equation which reads

$$\frac{\mathrm{d}^2\theta(\zeta)}{\mathrm{d}\zeta^2} - q \sin 2\theta(\zeta) = 0. \tag{5}$$

Here, we have used the dimensionless variable $\zeta \equiv z/l$ and the parameter $q \equiv \widetilde{\varepsilon}_a V^2/8\pi K$ which denotes the ratio between the electric energy and the elastic energy densities; in this sense, it measures the coupling between the electric field and the nematic. Here $\widetilde{\varepsilon}_a$ is the low-frequency dielectric anisotropy and $V \equiv E_0 l$ is the applied voltage.

An obliquely incident light beam whose polarization is contained in the incidence plane $x-z$ (linearly P-polarized), impinges the nematic with an angle of incidence i as shown in Fig. 1. We shall assume that the intensity of the beam is low enough such that it does not distort the nematic's configuration. Thus, the dynamics of this optical field is described by the corresponding Maxwell's equations containing the dielectric tensor ε_{ij}, Eq. (3), which depends on θ. The procedure to solve these equations has been carried out in detail for a hybrid cell similar to the one considered here [5] and it was found that there is a regime (so-called second regime) for the angle of incidence i where the ray trajectory exhibits a caustic, that is, where it bends and remains inside the cell until it returns back towards the incidence substrate (see Fig. 1). This trajectory is given by [5]

$$\upsilon = \chi - \int_0^\zeta \mathrm{d}\eta \frac{\varepsilon_{xz} \mp p\sqrt{\varepsilon_\perp \varepsilon_\parallel}/\sqrt{\varepsilon_{zz} - p^2}}{\varepsilon_{zz}}. \tag{6}$$

In this equation the dimensionless variable $\chi \equiv x/l$ has been introduced and $p \equiv N_b \sin i$ is the ray component in the x direction. Here υ is a constant to be determined by the coordinates of the point of incidence of the beam, that is, it establishes an initial condition. The $\pm$ sign in Eq. (6) corresponds to a ray traveling with $\mathbf{k}$ in the $\pm z$ direction, that is, going from A to B and from B to C, respectively, where the point B is the turning point and whose penetration length is ζ_c (see Fig. 1).

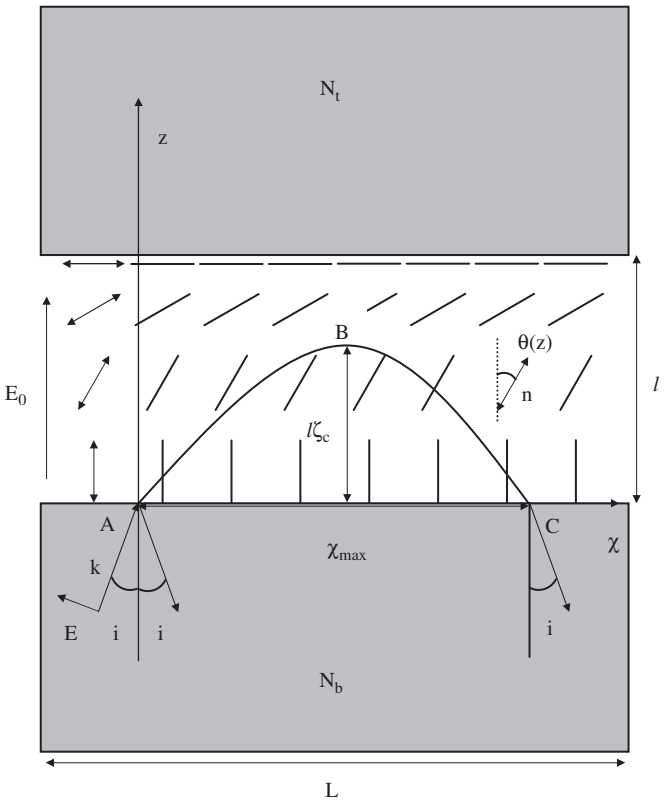

Fig. 1. Illustration of a pure thermotropic nematic confined between two parallel substrates. A P-polarized mode is traveling along the hybrid nematic. $N_b, N_t > n_\parallel, n_\perp$. The trajectory of the beam shows a caustic. ζ_c is the ray penetration. We have introduced the dimensionless variables $\zeta \equiv z/l$ and $\chi \equiv x/l$.

The steady-state orientational configuration is found by solving Eq. (5) subjected to the boundary conditions given by Eqs. (2). Numerically, we realize this by using the "shooting" method [6], in which a search for initial conditions consistent with the original boundary conditions is performed. The results for the orientational configuration are shown in Ref. [3].

As explained in [4], there are two regimes for i. The first one corresponds to $i - i_c < 0$, with i_c a critical angle, where all the rays always reach the top substrate and part of the ray is transmitted to the top plate. On the other hand, the second regime corresponds to $i - i_c > 0$, namely, when the ray does not reach the top substrate and it is reflected back to the inner of the cell as depicted in Fig. 1. Besides i_c, there is a second critical angle, i_{c2}, for which the beam no longer penetrate the liquid-crystal cell and it is reflected back to the lower substrate. Here we will consider only angles in the interval $i_c < i < i_{c2}$ for which the ray penetrates the cell and is reflected back.

We are interested in analyzing the influence that the wavelength dependence of the refractive index of the nematic has on the parameters of the trajectory. To that end, we utilize the refractive index correlations for 5CB at $T = 25.1\,^{\circ}\mathrm{C}$, obtained by fitting a three-band model and given by [7]

$$n_{\parallel} \cong 1 + n_{0\parallel} + g_{1\parallel}\left[\frac{\lambda^2\lambda_1^2}{\lambda^2-\lambda_1^2} + m_{\parallel}\frac{\lambda^2\lambda_2^2}{\lambda^2-\lambda_2^2}\right], \tag{7}$$

$$n_{\perp} \cong 1 + n_{0\perp} + g_{1\perp}\left[\frac{\lambda^2\lambda_1^2}{\lambda^2-\lambda_1^2} + m_{\perp}\frac{\lambda^2\lambda_2^2}{\lambda^2-\lambda_2^2}\right]. \tag{8}$$

The parameters appearing in the above equations are temperature dependent, but do not depend on the wavelength and are given by: $m_{\parallel} = g_{2\parallel}/g_{1\parallel}$, $m_{\perp} = g_{2\perp}/g_{1\perp}$, $\lambda_1 = 210\,\mathrm{nm}$, $\lambda_2 = 282\,\mathrm{nm}$, $g_{1\parallel} = 2.3250 \times 10^{-6}\,\mathrm{nm}^{-2}$, $g_{2\parallel} = 1.3970 \times 10^{-6}\,\mathrm{nm}^{-2}$, $n_{0\parallel} = 0.4552$, $g_{1\perp} = 1.3515 \times 10^{-6}\,\mathrm{nm}^{-2}$, $g_{2\perp} = 0.4699 \times 10^{-6}\,\mathrm{nm}^{-2}$, and $n_{0\perp} = 0.4136$. The resulting refractive indexes are plotted in Fig. 2.

The director's angle at the turning point, θ_c, is given by

$$\theta_c = \arccos\sqrt{(p^2 - \varepsilon_{\perp})/\varepsilon_a}, \tag{9}$$

from which the critical angles, i_c and i_{c2} can be obtained by substituting $\theta_c = 90^{\circ}$ and $\theta_c = 0^{\circ}$, respectively. In Fig. 3, we plot the critical angles as a function of λ. We can observe that the angular interval for which there are trajectories in the interior of the cell that reflect back, reaches its maximum for a wavelength near 400 nm and vanishes approximately for 300 nm. However, we are concerned in an angle for which there is a large bandwidth in which the trajectories reflect back to the inner part of the cell. Therefore, in order to obtain a large bandwidth within the second regime, we have chosen an arbitrary angle of incidence: $i = 64.5^{\circ}$ that we shall use in all our calculations. This angle is depicted by the dashed line in Fig. 3. The other parameters used in the figures are $N_b = N_t = 1.81$.

In Fig. 4 we show the trajectories of the beams calculated from Eq. (6), for $q = 0$, 0.75, 2, and 10. We notice the dispersion effect due to the wavelength dependence of the refractive indexes and that these trajectories are modified by changing the applied electric field. In this figure we show only the portion of the trajectory inside the nematic. Once the rays are refracted in the lower substrate they come out parallel as depicted in Fig. 1.

The range of a bending ray, χ_{max}, can be calculated from Eq. (6) by setting $\theta = 0$. This is shown in Fig. 5a where we have plotted the range as a function of q and λ. We observe a nonmonotonic behavior. That is, for q close to 0 the range is larger for shorter wavelengths and smaller for longer wavelengths whereas for a larger magnitude of the field, the dependence is inverted, i.e., the range is larger for longer wavelengths and smaller for shorter wavelengths. For intermediate values of q there is a crossover between these two cases and it appears a region where there is a superposition of waves with different wavelengths.

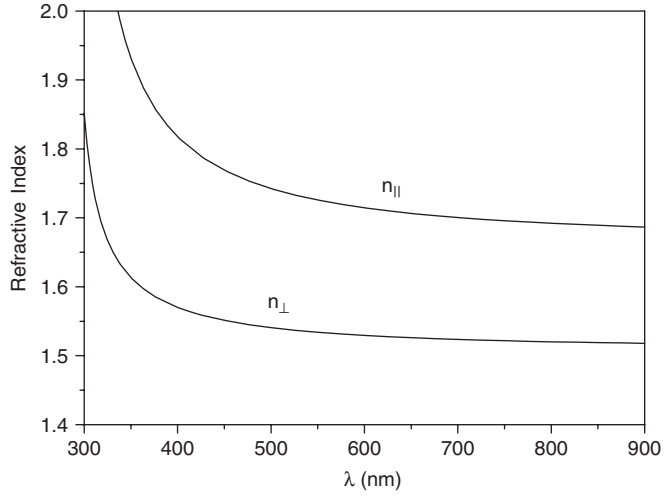

Fig. 2. Refractive index as a function of the wavelength of 5CB at $T = 25.1\,^{\circ}\mathrm{C}$.

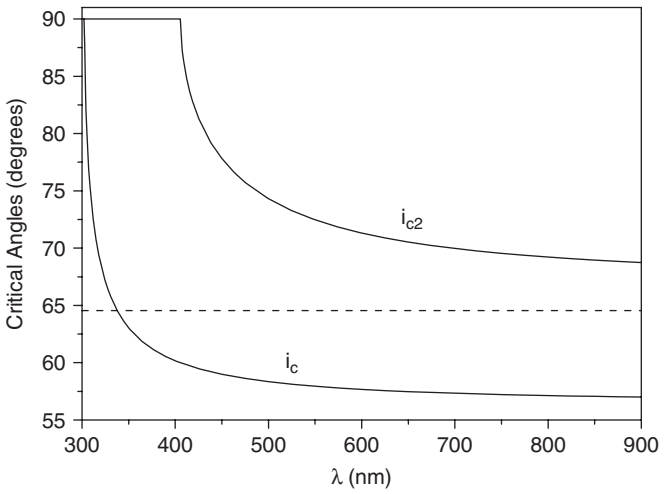

Fig. 3. Critical angles as a function of the wavelength.

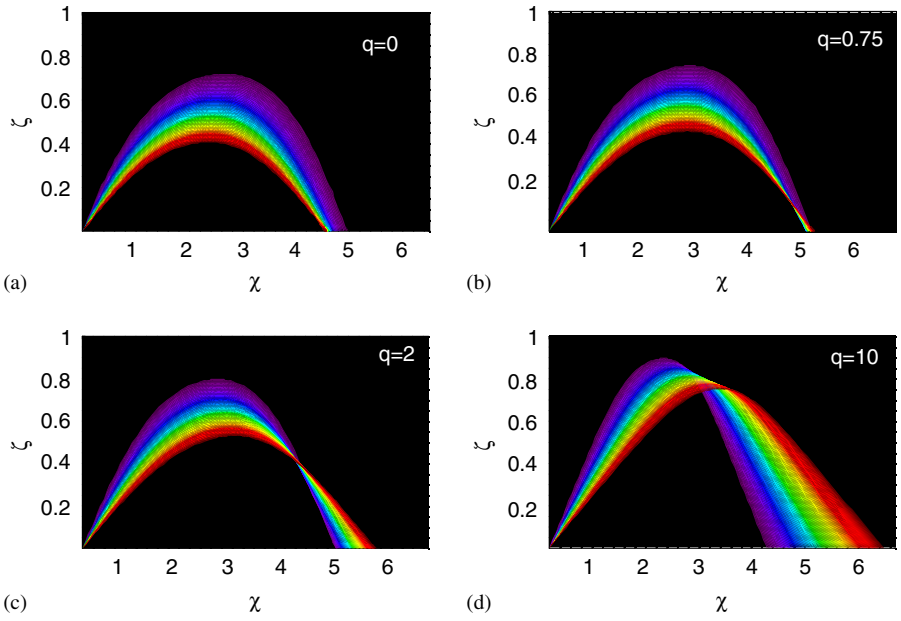

Fig. 4. Trajectories of the rays for the angle of incidence $i = 64.5°$. Four cases are shown, $q = 0$, 0.75, 2, and 10.

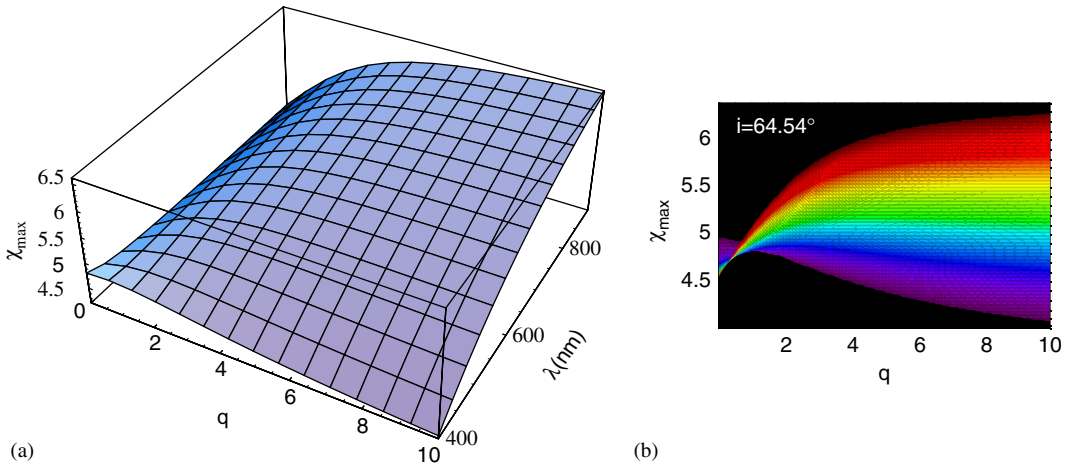

Fig. 5. (a) Dimensionless range of a bending ray χ_{max} as a function of q and λ, for the angle of incidence $i = 64.5°$. (b) Dimensionless range of a bending ray χ_{max} as a function of q, for the angle of incidence $i = 64.5°$.

In Fig. 5b we show the same information in a colorful presentation. Finally, in Fig. 6 we plot the derivative of the range as a function of λ, $d\chi_{max}/d\lambda$, for different values of q. This quantity is an important parameter to characterize the spatial resolution of the electrically controlled dispersion which plays the role of the angular resolution for a prism system. The key feature of our system is that, in contrast with the case of the prism, all the outgoing rays with different wavelength are parallel to each other. This is a convenient characteristic that could simplify the design of a multiplexor.

3. Conclusions

In summary, we have calculated the optical path for a linearly *P*-polarized beam traveling in a hybrid nematic cell subjected to a low-frequency electric field perpendicular to the cell. We have considered in detail the influence of the wavelength dependence of the refractive index, on the beam trajectories. Our results show that the range and the penetration length depend on the color of the beam and that these parameters can be controlled by varying the intensity of the applied electric field.

This phenomenon could be used for the design of optical devices. For instance, it is usual to combine this hybrid cell with an hemisphere of the same refractive index as the plate of incidence in order to eliminate the additional refraction in the plate–air interface, as shown in Ref. [4]. In this configuration, the output beam can be steered by a refraction process at the hemisphere–air interface since the reflected beam will emerge far from the center of the hemisphere. It should be remarked that we expect that

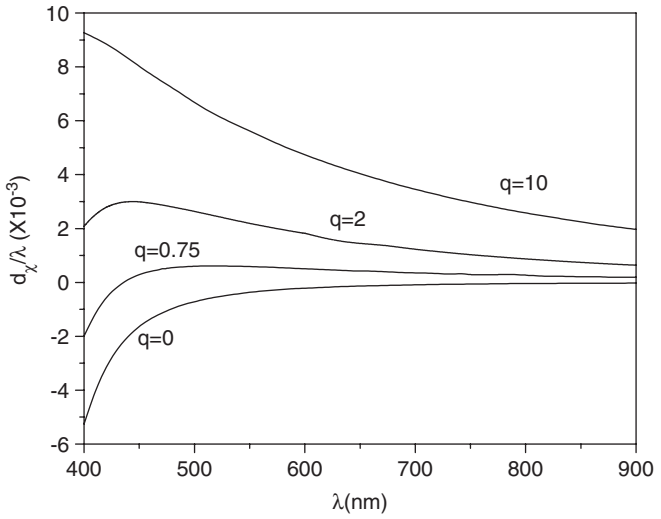

Fig. 6. Derivative of χ_{max} with respect to λ as a function of λ for $q = 0$, 0.75, 2, and 10.

most of the optical energy will be contained in this ray because the angle of incidence is far from the critical angle between the homeotropic layer and the substrate.

Another possible application consists in using this nematic cell as a multiplexor for switching among various optical fibers. This is due to the fact that the beam's range can be electrically controlled. The cell can be used to locate the outgoing beam in various cell's positions where some optical fibers were previously coupled. It should be stressed that the fact that the beam's output angle does not change by varying the applied voltage, simplifies considerably the optical coupling procedure with the output fibers.

Acknowledgments

This work was supported in part by Grants DGAPA-UNAM IN117606-3 and IN110103-3.

References

[1] M. Born, E. Wolf, Principles of Optics, Cambridge University Press, Cambridge, 1999.
[2] J. Chen, P.J. Bos, H. Vithana, D.L. Johnson, Appl. Phys. Lett. 67 (1995) 2588.
[3] C.I. Mendoza, J.A. Olivares, J.A. Reyes, Phys. Rev. E 70 (2004) 062701.
[4] J.A. Olivares, R.F. Rodriguez, J.A. Reyes, Opt. Commun. 221 (2003) 223.
[5] J.A. Reyes, R.F. Rodriguez, Mol. Cryst. Liquid Cryst. 317 (1998) 135.
[6] W.H. Press, B.P. Flannery, S.A. Teukolsky, W.T. Vetterling, Numerical Recipes in Fortran, second ed., Cambridge University Press, Cambridge, 1992.
[7] I.C. Khoo, Liquid Crystals: Physical Properties and Nonlinear Optical Phenomena, Wiley, New York, 1994.